Modeling and Simulation of a Torque Controlled Permanent Magnet Synchronous Motor Drive

Jyoti Agrawal
Department of Electrical Engineering
G. H. Raisoni College of Engineering
Nagpur, India

Sanjay Bodkhe
Department of Electrical Engineering
Shri Ramdeobaba College of Engineering & Management
Nagpur, India

***Abstract*—This paper presents the detailed modeling and simulation of a permanent magnet synchronous Motor (PMSM) drive system. The torque control of PMSM is achieved with the help of vector control, which is the widely accepted method. It provides independent control of torque and mutual flux. The switching signals for inverter are generated by two techniques to test their effect for superior performance of the drive. They are hysteresis and sinusoidal pulse width-modulation (PWM) with current control. The response of the two drives are studied by simulation and evaluated based upon the magnitude of current ripples and torque pulsation. Also the effect on Total harmonic distortion (THD) which is a measurement of harmonic distortion or harmonic components of a distorted waveform is investigated. The proposed drive is tested at various operating conditions to conclude the effect of different switching techniques on the drive system. The study is carried out with Matlab Simulink software.**

Keywords—Mathematical model; vector control; torque control; PMSM drive; MATLAB/Simulink.

NOMENCLATURE

B	damping constant, (N/rad/s)
f_c	carrier frequency, (Hz)
H	inertial constant in normalized unit, (p.u.)
i_{ds}, i_{qs}	*d*- and *q*-axes stator currents in stator reference frame, (A)
i^r_{ds}, i^r_{qs}	*d* and *q*-axes stator currents in rotor reference frame,(A)
i^*_{as}, i^*_{bs}, i^*_{cs}	command stator phase currents, (A)
i_{as}, i_{bs}, i_{cs}	instantaneous stator phase currents, (A)
i^*_s	stator current reference, (A)
J	total moment of inertia, (kg-m^2)
L_{dd}, L_{qq}	stator *d* and *q*-axes self-inductances in stator reference frame, (H)
L_{dq}, L_{qd}	mutual inductances between *d*- and *q*- axes windings, (H)
L_d, L_q	stator *d*- and *q*-axes self-inductances in rotor reference frame, (H)
P	number of poles
R_d, R_q	stator *d*- and *q*-axes winding resistances, (Ω)
R_s	stator resistance per phase, (Ω)
T_b	base torque, (N-m)
T_e	electromagnetic torque, (N-m)
T_e^*	torque reference, (N-m)
T_l	load torque, (N-m)
v_{ds}, v_{qs}	*d*- and *q*-axes stator voltages in stator reference frame, (V)
v^r_{ds}, v^r_{qs}	d- and q-axes stator voltages in rotor reference frame, (V)
v_{ao}, v_{bo}, v_{co}	inverter midpole voltages, (V)
v_{as}, v_{bs}, v_{cs}	input phase voltages, (V)
λ_{ds}, λ_{qs}	*d*- and *q*-axes stator flux linkages, (Wb)
λ_{af}	armature flux linkages, (Wb)
λ^*_m	reference mutual air gap flux linkages, (V-s)
p	differential operator, d/d*t*
θ_r	rotor position, (radians)
θ^*_s	stator current command phase angle, (rad)
ω^*_r	speed reference, (rad/s)
ω_r	actual rotor speed, (rad/s)
δ	torque angle, (rad)
δ^*	torque angle command, (rad)
Δi	hysteresis current window, (A)

I. INTRODUCTION

Recently, an increased interest in application of permanent magnet synchronous motors (PMSM) in industry for industrial drive application has been observed due to numerous advantages [1]-[5]. Permanent magnet synchronous machine has overcome the limitations of synchronous motor by using the high energy permanent magnet like Neodymium-Iron-Boron (NdFeB) instead of electromagnets [4]. The use of permanent magnet has replaced the need of slip rings required for field excitation which results in low maintenance and low losses in the rotor [2]. From literature, it is apparent that for operation of PMSM under closed loop there exist different techniques [2], [6]-[9]. For proper operation of a PMSM it is necessary to determine the exact rotor position. Commonly, a position sensor, such as optical encoder, Hall Effect sensor or resolver, is fitted to for sensing the rotor position [1]. The vector control of PM motors is much simpler than that of induction motors (IM) because there is no need to consider the slip frequency as in IM drive [7]. This paper describes a simple torque control method for a PMSM drive that provides a high-performance vector control. By using the proposed model, pulse width-modulated (PWM) current controlled inverter fed PMSM torque drive is simulated in Matlab Simulink environment and the results are then compared with those obtained by using hysteresis current controlled inverter fed PMSM torque drive. In the torque control scheme, three phase currents are regulated by using hysteresis/PWM current controllers, which operate in the rotor reference frame. Before switching the inverter, the modified current errors are transformed to the stator phase currents by inverse Park transformation using measured rotor

position from an encoder [4]. Torque controlled drive system utilizes PMSM model to predict the voltage required for achieving a desired output torque. The dynamic model of PMSM can be derived to evaluate the instantaneous effects of varying current, voltage, stator frequencies and torque disturbance on the performance of machine and drive system [3]. It has been seen from most of the earlier research works that the concept of switching function is a powerful tool which helps in understanding and optimizing the performance of the static power converters/inverters [10, 11]. In this paper a functional simulation model for the voltage source inverter (VSI) fed PMSM using the switching function concept is studied and implemented in Matlab Simulink. The desired performance is achieved by implementing vector control technique (normally used in ac machines so as to provide decoupling between torque and flux producing components) in Matlab/Simulink and tested under different operating conditions [8]. The main aim of this drive system is to have torque control by controlling the torque angle (δ) and the magnitude of current phasor (i_s) [3]. Due to the implementation of functional modeling, the developed models have various advantages [11].

The torque controlled PMSM drive system is tested under different operating conditions such as load torque disturbance, speed reversal, reduction in torque ripple, varying switching frequency, change in hysteresis current window and change in PWM carrier frequency etc. and the simulation results are presented. In addition to this study effects due to the use of (PWM) and hysteresis current controllers on the torque pulsation of motor and drive performance are also evaluated. The main drawback of torque controlled PMSM drive using inverter with hysteresis current control is fast sampling time required and variable switching frequency [12]. Hence, in order to eliminate above disadvantages a new developed control technique called torque control with PWM current control has been introduced [13].

This paper is divided into seven sections. Section 1 provides a general introduction and literature review of the PMSM. In section 2, the dynamic modeling of the PMSM is presented. Section 3 contains model of PMSM in the form of Simulink model. Section 4 contains a study of vector control control strategy of PMSM. Section 5 presents a newly developed torque controlled PMSM drive in the form of Simulink model. Section 6 has the simulation results. Also, a comparative evaluation of hysteresis and PWM current controller designs used in the proposed PMSM, based upon the magnitude of current ripple and the torque pulsation is presented in this section. The paper is concluded in section 7.

The proposed functional modeling of PMSM enables to have an insight into the behavioral characteristics of the machine under different operating conditions.

II. DYNAMIC MODEL OF PMSM

The detailed modeling of three phase PMSM drive system is required for proper simulation and analysis of the system. The model of the PMSM is developed using a two- phase configuration along direct and quadrature axes. This provides simplicity of only one set of windings on the stator. The rotor has no windings but consists of permanent magnets only [3], [4]. The model developed for the PMSM drive is using the following assumptions [14].

- The saturation effect and changes in parameters are neglected.
- The inductance versus rotor position is sinusoidal.
- The stator windings are balanced with sinusoidally distributed magnetomotive force.
- Windage, friction and drive losses are ignored.

With the above assumptions, the *d*- and *q*-axes stator voltages in rotor reference frame are:

$$\begin{bmatrix} v_{qs}^{r} \\ v_{ds}^{r} \end{bmatrix} = \begin{bmatrix} R_s + L_q p & \omega_r L_d \\ -\omega_r L_q & R_s + L_d p \end{bmatrix} \begin{bmatrix} i_{qs}^{r} \\ i_{ds}^{r} \end{bmatrix} + \begin{bmatrix} \omega_r \lambda_{af} \\ 0 \end{bmatrix} \quad (1)$$

From (1), it is observed that the voltage equations are equal to the product of the impedance matrix and the current vector, plus an additional component due to the motional emf of the rotor flux linkages. Electromagnetic torque is the most important variable as it determines the rotor position and speed. The expression for the electromagnetic torque developed by the machine can be expressed in d- and q-components of the currents as,

$$T_e = \frac{3}{2}\frac{P}{2}\left[\lambda_{af} + \left(L_d - L_q\right) i_{ds}^{r}\right] i_{qs}^{r} \quad (2)$$

Equation (3) represents the electromechanical dynamic equation.

$$T_e = J\frac{d\omega_m}{dt} + T_l + B\omega_m \quad (3)$$

The stator phase voltages are obtained from (1) by using the inverse Park transformation as,

$$\begin{bmatrix} v_{as} \\ v_{bs} \\ v_{cs} \end{bmatrix} = \begin{bmatrix} \cos\theta_r & \sin\theta_r & 1 \\ \cos\left(\theta_r - \frac{2\pi}{3}\right) & \sin\left(\theta_r - \frac{2\pi}{3}\right) & 1 \\ \cos\left(\theta_r + \frac{2\pi}{3}\right) & \sin\left(\theta_r + \frac{2\pi}{3}\right) & 1 \end{bmatrix} \begin{bmatrix} v_{qs}^{r} \\ v_{ds}^{r} \\ v_0 \end{bmatrix} \quad (4)$$

Similarly, the *dqo* currents are obtained from *abc* currents using Park transformation as,

$$\begin{bmatrix} i_{qs}^{r} \\ i_{ds}^{r} \\ i_0 \end{bmatrix} = \begin{bmatrix} \cos\theta_r & \cos\left(\theta_r - \frac{2\pi}{3}\right) & \cos\left(\theta_r + \frac{2\pi}{3}\right) \\ \sin\theta_r & \sin\left(\theta_r - \frac{2\pi}{3}\right) & \sin\left(\theta_r + \frac{2\pi}{3}\right) \\ \frac{1}{2} & \frac{1}{2} & \frac{1}{2} \end{bmatrix} \begin{bmatrix} i_{as} \\ i_{bs} \\ i_{cs} \end{bmatrix} \quad (5)$$

In a balanced three-phase system, the sum of three phase currents is zero, leading to i_0 of zero value. Hence, if any two phase currents are measured, the third-phase current can be obtained by algebraic manipulation of the other two-phase currents. This eliminates the need for additional current sensors.

In order to have a meaningful interpretation in the modeling, analysis and simulations, the power input to the three phase machine has to be equal to the power input to the two phase machine. From (1) and (3) the complete dynamic model of PMSM in rotor reference frame is derived and is expressed by (6).

$$p\begin{bmatrix} i_{qs}^{r} \\ i_{ds}^{r} \\ \omega_r \\ \theta_r \end{bmatrix} = \begin{bmatrix} -\frac{R_s}{L_q} & -\frac{L_d}{L_q}\omega_r & -\frac{\lambda_{af}}{L_q} & 0 \\ \frac{L_q}{L_d}\omega_r & -\frac{R_s}{L_d} & 0 & 0 \\ \frac{\lambda_{af}}{2H} & \frac{-(L_d-L_q)i_{qs}^{r}}{2H} & \frac{-B}{2H} & 0 \\ 0 & 0 & 1 & 0 \end{bmatrix} \begin{bmatrix} i_{qs}^{r} \\ i_{ds}^{r} \\ \omega_r \\ \theta_r \end{bmatrix} + \begin{bmatrix} \frac{1}{L_q} & 0 & 0 \\ 0 & \frac{1}{L_d} & 0 \\ 0 & 0 & -1 \end{bmatrix} \begin{bmatrix} v_{qs}^{r} \\ v_{ds}^{r} \\ T_l \end{bmatrix} \quad (6)$$

Equation (6) is used for the simulation of PMSM model. It gives the information of rotor position which is of crucial importance in determining the current and voltage in each phase of the machine.

III. SIMULATION OF PMSM

The functional model of PMSM is built in several steps through the construction of d- and q-axes stator currents in rotor reference frame, electromagnetic torque, rotor speed and rotor position.

A. *d-q axis stator current in rotor reference frame*

By using (6), the d-axis and q-axis model is constructed as shown in Fig. 1 and Fig. 2 respectively.

B. *Electromagnetic torque*

The electromagnetic torque T_e developed on the rotor can be obtained as given by (7). From (7), it is seen that the torque of PMSM can be calculated in terms of the estimated stator flux linkage and motor current [15].

$$T_e = \frac{3}{2}\frac{P}{2}\left[\left(L_d - L_q\right)i_{ds}^{r} + \lambda_{af}\right]i_{qs}^{r} \quad (7)$$

C. *Rotor position*

To implement vector controlled PMSM drive system the information of rotor position is necessary. The speed of the machine is maintained at a certain speed. By using (6) the rotor position (θ_r) is calculated.

IV. VECTOR CONTROL LED PMSM TORQUE DRIVE

Control of PMSM is based on the information of rotor position and speed which has been always a challenging task. The main problem lies in accurate and rapid estimation of rotor position [16]. Various types of closed-loop control techniques are proposed and validated for PMSM, like scalar and vector control [2]. The vector control method allows to change and control stator currents or voltage both in magnitude and phase at the same time which helps in achieving high dynamic performance. A proposed vector control scheme for PMSM is shown in Fig. 3. The first block is current and torque angle calculator, here in this block using Te* and λ*m, the i*s and δ* signals are calculated. The next block is the stator reference current synthesizer where reference current signals are generated by using Equations (12)-(14). The rotor position is sensed by using a position transducer. On comparing the respective reference current to the actual phase current switching pattern for the power devices are produced [17]. The most popular vector control is known for decoupling as it allows independent control of torque and mutual flux from each other [18]. Vector control to PMSM is normally used to get the control, in the same way as that of the separately excited dc motor, which has high desirable control characteristics [18]. The vector control can be implemented either by using Field Oriented Control (FOC) or Direct Torque Control (DTC) [19]. By using (7), the electromagnetic torque in PMSM can be expressed as,

$$T_e^{*} = \frac{3}{2}\frac{P}{2}\left[\lambda_{af} i_s^{*}\sin\delta^{*} + \frac{1}{2}\left(L_d - L_q\right)\left(i_s^{*}\right)^2 \sin 2\delta^{*}\right] \quad (8)$$

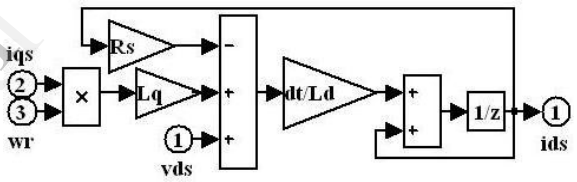

Fig. 1. Simulink model for i^{r}_{ds}

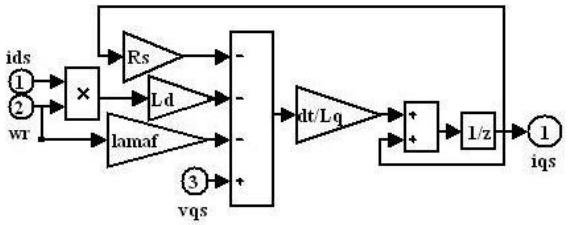

Fig. 2. Simulink model for i^{r}_{qs}

$$\alpha + \beta = \chi. \quad (1) \quad (1)$$

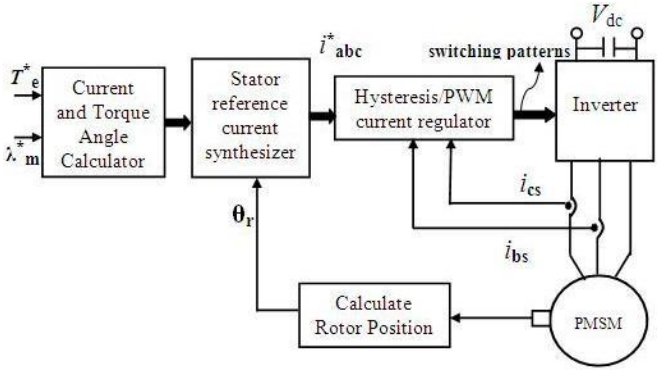

Fig. 3. Proposed vector controlled PMSM drive□□□□□□□□

In (8) if δ is assumed to be zero, then the expression for torque of PMSM becomes similar to torque of separately excited dc machine. The magnitude of reference mutual flux linkage is given by (9).

$$\lambda_m^* = \sqrt{\left(\lambda_{af} + L_d i_s^* \cos\delta^*\right)^2 + \left(L_q i_s^* \sin\delta^*\right)^2} \qquad (9)$$

The stator current phase angle command is obtained by summing the rotor position and torque angle as given by (10).

$$\theta_s^* = \theta_r + \delta^* \qquad (10)$$

V. IMPLEMENTATION OF VECTOR-CONTROLLED PMSM TORQUE DRIVE

The vector controlled PMSM torque drive is implemented using the software Matlab/Simulink. By combining Fig. 1, 2 and Fig. 5 to Fig. 8 the complete torque drive for PMSM fed from Hysteresis/PWM current control inverter has been developed as shown in Fig. 4. It consists of five functional blocks. They are current and torque angle calculator, stator current synthesizer, inverter with hysteresis/PWM current control, PMSM model and signal conditioner. A PMSM drive with external inputs of torque and mutual flux linkages known as references are considered. The actual phase currents are firstly calculated based on the PMSM model and in the third functional block which is hysteresis/PWM current regulator, here the calculated phase currents are compared with the references. The outputs of the comparators are the switching signals which are used to select the appropriate stator voltage vector so as to minimize the current errors [11, 20].

The stator windings of the PMSM are fed by a PWM/Hysteresis current controlled inverter which controls the torque and mutual flux linkages directly. An inverse Park transformation is used which transforms the two-phase signals into three-phase which are then used as feedback as shown in the scheme. The reference torque angle (δ) can be obtained from (8) and (11) assuming the machine parameters to be constants. Each functional block is elaborated in detail in the following sections.

$$\alpha + \beta = \gamma \qquad (1) \qquad (1)$$

A. Current and torque angle Calculator

If the rotor has a surface mounted design (SMPMSM), where $L_d = L_q$, then the stator current reference obtained from the expression in (9) is given as

$$i_s^* = \frac{\sqrt{\left(\lambda_m^*\right)^2 - \lambda_{af}^2 - 2\lambda_{af}\left(i_s^* \cos\delta^*\right)}}{L_d} \qquad (11)$$

This is shown in Fig. 5. The torque reference value of 5.5631 Nm and the flux linkage reference with 0.1546 V-s is put on the motor drive [14]. The process of obtaining current (i_s^*) and torque angle (δ^*) by using (8) and (9) is the heart of vector controller [4, 14, 21].

B. Reference currents

The reference currents are generated by using (12)-(14).

$$i_{as} = i_s \sin\left(\omega_r t + \delta\right) \qquad (12)$$

$$i_{bs} = i_s \sin\left(\omega_r t + \delta - \frac{2\pi}{3}\right) \qquad (13)$$

$$i_{cs} = i_s \sin\left(\omega_r t + \delta + \frac{2\pi}{3}\right) \qquad (14)$$

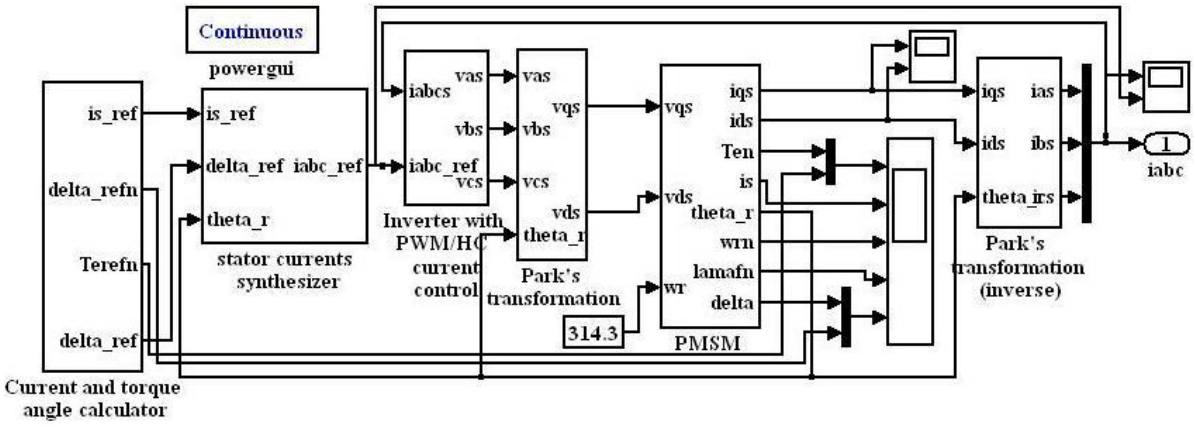

Fig. 4. Block diagram of simulation model for inverter fed vector-controlled PMSM torque drive using hysteresis/PWM current control

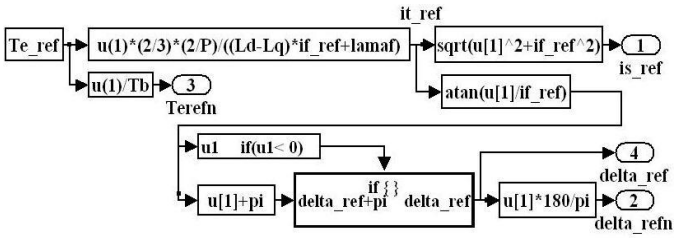

Fig. 5. Current (i^*_s) and torque angle (δ^*) calculator block

C. Current Controlled Inverter Model

Fig. 4 show that the PMSM is fed from a voltage source inverter with current control. A comparative study is carried out by using two different current controllers to generate gate signals for the inverter i.e. Pulse Width Modulation (PWM) and Hysteresis Current Controller. Proper selection of the inverter power devices (such as IGBT, MOSFET, GTO etc.) and selection of the current control technique will guarantee in improving the efficiency of the drive [20, 22].

D. Pulse Width Modulation Current Controller

Sinusoidal pulse width modulation (SPWM) is the most commonly used technique for controlling inverter output voltage and harmonic reduction. The Simulink model of SPWM current control strategy for phase a is shown in Fig. 6.

The functional model of a three phase PWM current controlled inverter is shown in Fig. 7. The error of the controlled signal is then compared against a common high frequency triangular carrier wave of desire switching frequency. The comparison will result in a pulse when the error signal is greater than the triangular wave which is then used to trigger the respective power devices [23]. The speed at which inverter switches are turned on and off depends on the switching frequency is usually fixed at carrier frequency (fc).

The output line-to-line voltages can be defined by following equations

$$v_{ab} = v_{ao} - v_{bo},\ v_{bc} = v_{bo} - v_{co} \text{ and } v_{ca} = v_{co} - v_{ao} \quad (15)$$

Assuming the system to be balanced the phase voltages are computed in terms of line-to-line values with the help of (16) [2, 24, 25].

$$v_{as} = \frac{v_{ab} - v_{ca}}{3},\ v_{bs} = \frac{v_{bc} - v_{ab}}{3} \text{ and } v_{cs} = \frac{v_{ca} - v_{bc}}{3} \quad (16)$$

The three-phase voltages of the inverter are converted to two-phase by using Park transformation (refer (4) and (5)).

E. Hysteresis Current Controller

The basic implementation of hysteresis current control technique is based on deriving the switching patterns to the inverter from the comparison of the current error within a fixed hysteresis band [26]. The inverter midpole voltage is determined by the logic given in (17). The hysteresis current control keeps the actual value of the currents within the specified bands all the time. The hysteresis window Δi, can be set externally. In this controller the reference current of a respective phase is summed with the negative of the actual or measured current. The error thus obtained of respective phase is then fed to a comparator having a tolerance band around the reference current associated with that phase. The hysteresis current controller reacts instantaneously to changes in the current command; hence there is no delay [27]. The benefits of hysteresis current controllers are good accuracy, simple design and high robustness. The major drawback with this controller is that it does not have a fixed switching frequency as in PWM current control and varies continuously but it is related with the Δi. Simulink model is shown in Fig. 8.

$$\begin{aligned} &\text{if} \quad \left(i^*_{as} - i_{as}\right) \geq \Delta i, \ \text{set} \ v_{ao} = \frac{V_{dc}}{2} \\ &\text{else if} \left(i^*_{as} - i_{as}\right) \leq -\Delta i, \ \text{set} \ v_{ao} = -\frac{V_{dc}}{2} \end{aligned} \quad (17)$$

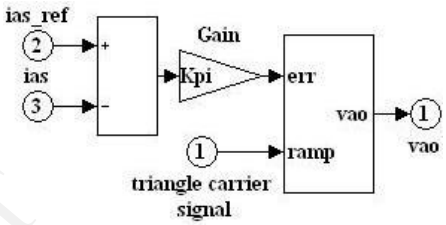

Fig. 6. Simulink model of SPWM current control strategy for phase a

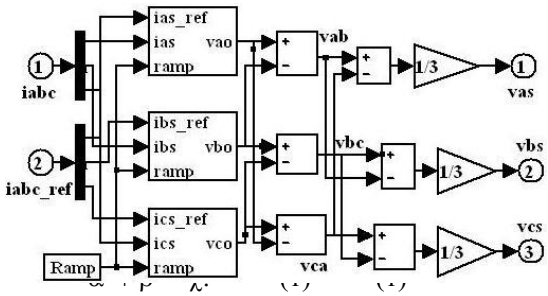

Fig. 7. Simulink model of PWM current controlled inverter

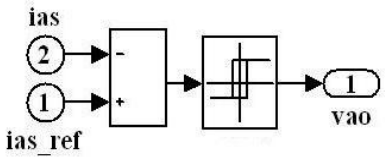

Fig. 8. Simulink model of Hysteresis current controlled inverter

VI. SIMULATION RESULTS AND DISCUSSION

To study the performance of torque-controlled PMSM drive system using hysteresis/PWM current control the simulation model has been developed in MATLAB environment. The behavior of torque-controlled system is analyzed and the response of PMSM is observed for load torque disturbance, speed reversal, reduction in torque ripple,

varying switching frequency, change in hysteresis current window and change in PWM carrier frequency etc. The simulation is carried out using two current control methods i.e. hysteresis and PWM to study the performance of PMSM drive system. The plots of torque, speed, current and flux linkage are given for all the cases. From the simulation results it is observed that the commanded torque is tracked very well (refer Fig. 9 to Fig. 11 and Fig. 13 to Fig. 15). The plotted variables are in normalized units (p.u.). The parameters for PMSM are given in the appendix. In all the simulations rated speed of 628.6 rad/s is selected as base speed.

A. Vector-Controlled PMSM Torque Drive with Hysteresis current control

The torque controlled PMSM drive is tested under different operating conditions as follows (a) change in load torque (b) speed reversal (c) change in hysteresis current window.

Fig. 9 to Fig. 11 reveal simulation results of the PMSM drive when fed through three-phase hysteresis current controlled inverter.

1) Disturbance in torque:

Fig. 9.a. gives the simulation results of the torque response of the PMSM under the condition of a step change of torque command. A torque of 0.4 p.u. is added and then increased to 1 p.u. at 0.005s. From Fig. 9.a. it can be seen that the torque response is very fast. In this test the motor speed is assumed constant, which is chosen as 314.3 rad/s and the hysteresis current window is set at 0.1 p.u. Simulated three phase currents are shown in Fig. 9.c. (reference) and Fig. 9.d.(actual) respectively.

2) Speed reversal:

Fig. 10 give the simulation results under the condition of applying constant amplitude of rotor flux linkage. Fig. 10.b. shows the response of speed of the PMSM under a step change of reference speed from 0.5 p.u. (314.3 rad/s) to -0.7 (-440 rad/s) p.u. at the time 0.005s. It is seen from Fig. 10.a. that the torque under any circumstances is able to follow the reference quite well. Fig. 10.a. shows the reference and actual torque. Mutual flux linkages increases with the increase in stator current magnitude (refer Fig. 10.d and Fig. 10.e). In this test test Δi is set at 0.3 p.u.

3) Change in hysteresis current window:

Fig. 11 reveals the torque and flux waveforms for three different hysteresis bands (Δi=4%, Δi=10% and Δi=20% respectively). Step change in reference torque is applied two times i.e. at 0.002 s, from 2 N-m (30% of the rated torque) to 5.5631 N-m (100% of the rated torque) and vice-versa at 0.0045 s. Torque and flux tracking performance analysis allows selection of the optimal hysteresis current window in accordance with the respective power switches.

4) Calculation of total harmonic distortion:

In Fig. 12 it is seen that the total harmonic distortion (THD) of current waveform for phase a under hysteresis current control technique is 21.6%. Table I shows the THD analysis for currents using the hysteresis current control technique for varying hysteresis bands. Table I shows that when the hysteresis band is selected as Δi=4%, it provides the lowest THD of 17.57 %, 20.22 %, 25.68 % for current of all the three phases i.e. a, b and c respectively.

TABLE I. THD ANALYSIS OF THE PMSM DRIVE USING HYSTERESIS CURRENT CONTROLLED INVERTER

Sr. No.	Hysteresis Current Control Technique		
	Hysteresis band (Δi)	*Phase*	*THD in current %*
1.	Δi = 0.48 p.u.	a	17.57
		b	20.22
		c	25.68
2.	Δi = 1.2 p.u.	a	21.6
		b	23.76
		c	28.49
3.	Δi = 2.4 p.u.	a	33.53
		b	35.07
		c	34.49

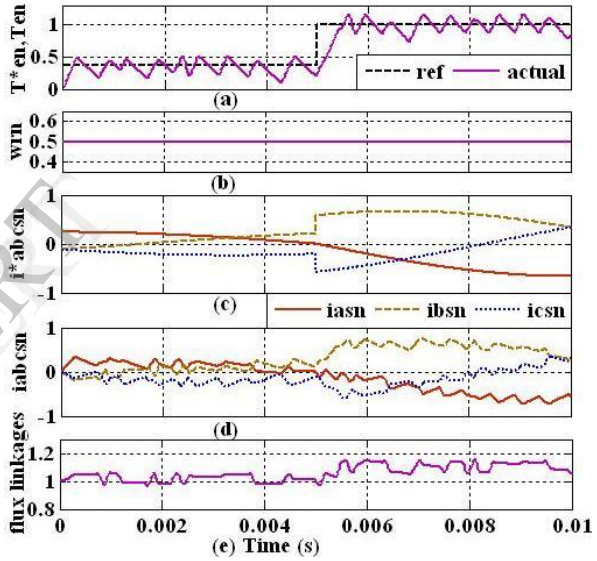

Fig. 9. Torque control of a PMSM with constant reference speed and step change of torque command 0.4 p.u. is added and then increased to 1 p.u. at 0.005s. (a) Torque response (b) Speed response (c) Reference phase currents response (i^*_{as}, i^*_{bs}, i^*_{cs}) (d) Phase current response (i_{as}, i_{bs}, i_{cs}). (e) Mutual flux linkages response.

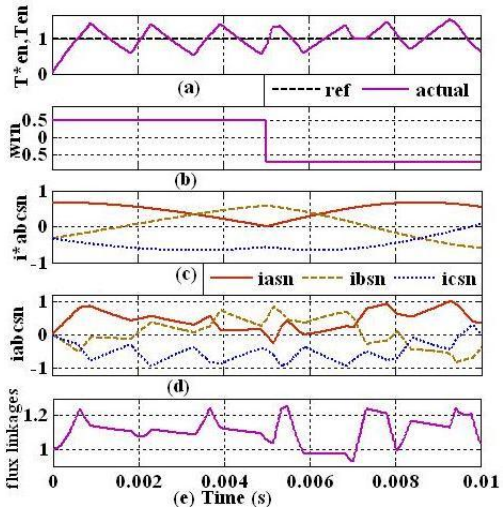

Fig. 10. Torque control of a PMSM with with step change in reference speed from 314.13 rad/s to -440 rad/s at 0.05s (a) Torque response (b) Speed response (c) Reference phase currents response (i^*_{as}, i^*_{bs}, i^*_{cs}) (d) Phase current response (i_{as}, i_{bs}, i_{cs}). (e) Mutual flux linkages response.

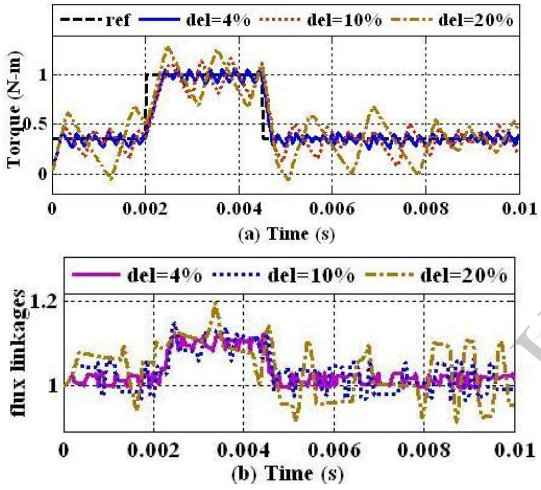

Fig. 11. Torque step and flux response for three different hysteresis bands (Δi=4%, Δi=10% and Δi=20% respectively). (a) Torque tracking performance (b) Flux tracking performance.

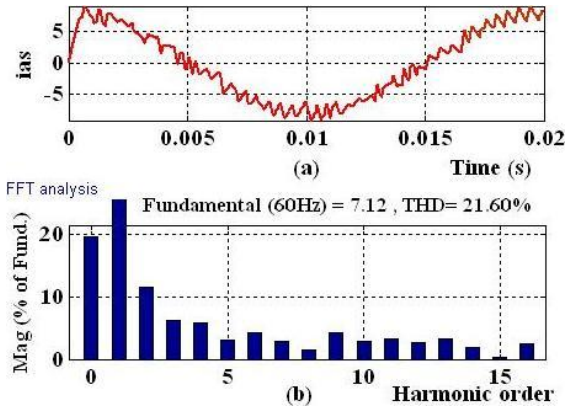

Fig. 12. Stator phase a current and its spectrum for hysteresis bands (Δi=10%) (a) phase a current waveform (b) current spectrum.

B. Vector-Controlled PMSM Torque Drive System with PWM current Control

Fig. 13 to Fig. 15, the simulation results are observed for torque, speed, motor currents and flux linkage for the PMSM drive when fed by PWM current control inverter instead of a Hysteresis current control inverter. The torque response in Fig. 13.a. shows considerable drop in torque and current ripples after using a PWM current controlled inverter.

1) Disturbance in torque:

In this test, the drive is operated with a constant speed and there is a step change in reference torque. At 0.005 s (see Fig. 13.a.), a motor reference torque is increased to 1 p.u. (5.5631 N-m). It is seen from Fig. 13.a. that the response of torque is improved. The increase in torque causes increase in stator current magnitude which in turn increases the mutual flux linkages [22]. (see Fig. 13.a, 13.d and 13.e).

2) Speed reversal:

In this test, the drive is analyzed with a disturbance in speed command that is the reference speed is step changed from 314.3 rad/s to -440 rad/s at 0.005 s, under constant load torque of 5.5631N-m. From figure 14.c and 14.d it is seen that in this test the phase sequence reverses to rotate the motor in reverse direction.

3) Change in carrier frequency:

Fig. 15 represents the motor actual torque response due to the torque controlled drive for change in carrier frequency. The torque step response and flux response for varying carrier frequency f_c =20 kHz, 10 kHz, 2.5 kHz is shown in Fig. 15. Also it is seen that the actual torque response contains ripples. In this test, step change in reference torque is applied two times i.e. at 0.002 s, from 2 N-m (30% of the rated torque) to 5.5631 N-m (100% of the rated torque) and vice-versa at 0.0045 s, as it is shown in Fig. 15.a.

4) Calculation of total harmonic distortion:

After using the SPWM current control technique, the THD is effectively reduced to 14.53% (when f_c =20 kHz) as shown in Fig. 16. The waveform of stator current for phase a is better than that obtained with hysteresis current controller (refer Fig. 12.a. and Fig. 16.a). Table II shows the THD analysis for currents using the PWM current control technique for two different carrier frequencies [28]. It also shows the comparison of THD levels for all the three phases.

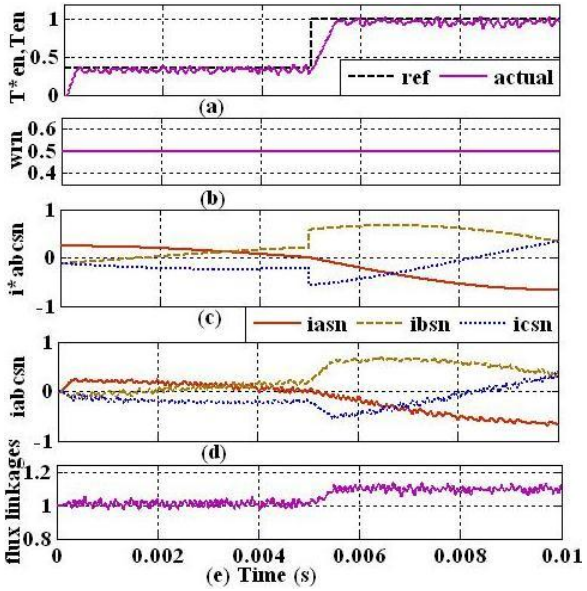

Fig. 13. Torque control of a PMSM with constant reference speed and step change of torque command 0.4 p.u. is added and then increased to 1 p.u. at 0.005s. (a) Torque response (b) Speed response (c) Reference phase currents response (i^*_{as}, i^*_{bs}, i^*_{cs}) (d) Phase current response (i_{as}, i_{bs}, i_{cs}). (e) Mutual flux linkages response.

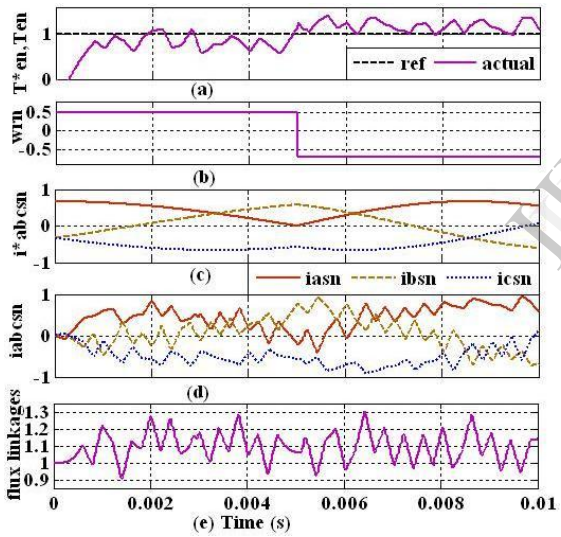

Fig. 14. Torque control of a PMSM with with step change in reference speed from 314.13 rad/s to -440 rad/s at 0.05s under constant load torque of 5.5631 N-m. (a) Torque response (b) Speed response (c) Reference phase currents response (i^*_{as}, i^*_{bs}, i^*_{cs}) (d) Phase current response (i_{as}, i_{bs}, i_{cs}). (e) Mutual flux linkages response.

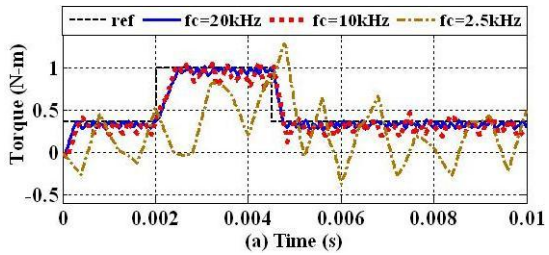

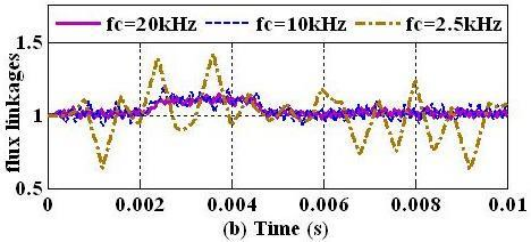

Fig. 15. Torque step and flux response for three varying carrier frequency (f_c =20 kHz, 10 kHz, 2.5 kHz respectively). (a) Torque tracking performance (b) Flux tracking performance.

TABLE II. THD ANALYSIS OF THE PMSM DRIVE USING PWM CURRENT CONTROLLED INVERTER

Sr. No.	SPWM Current Control Technique		
	Carrier frequency (f_c) kHz	*Phase*	*THD in current %*
1.	f_c = 2.5	a	27.54
		b	25.69
		c	15.42
2.	f_c = 20	a	14.53
		b	21.84
		c	18.69

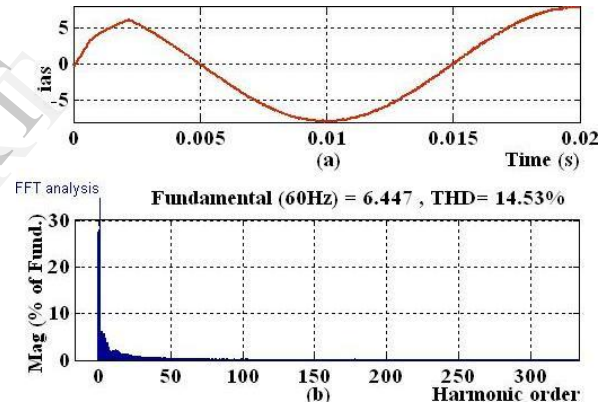

Fig. 16. Stator phase a current and its spectrum for carrier frequency (*f*c=20kHz) (a) phase a current waveform (b) current spectrum.

VII. CONCLUSION

The dynamic modeling and simulation study of PMSM drive using two different techniques for generation of switching signals is presented in this paper. A comparative evaluation based upon the ripple content in stator currents and torque pulsation is carried out to determine the effectiveness and performance wise superiority of hysteresis and sinusoidal PWM technique. The THD analysis of the PMSM drive for current waveform under both the techniques is presented. A comparison of THDs at various hysteresis bands and different carrier frequency is made and it has been concluded that THD under SPWM technique is lowest as compared to the hysteresis current control technique.

It is seen from the simulation results that the pulsation in torque, ripples in current and hence flux characteristics are considerably lower when the PWM current control technique is used as compared to the hysteresis current controller. Also it is concluded from the simulation results that whether a

PWM or hysteresis current controller is used on an average the nature of torque and flux linkages curve remains same. This study confirms that PWM current control technique is superior to hysteresis current controllers when compared with large hysteresis window. The main advantage of using hysteresis current controllers are good accuracy, simple design and high robustness. But the major drawback with this technique is that it does not have a fixed switching frequency as in PWM current control. Simulation results indicate that the proposed scheme is effective in obtaining fast torque response. The simulation results confirm that the design of vector controlled PMSM drive is valid. The general theory of switching functions was reviewed for implementing proposed function model.

REFERENCES

[1] I. Boldea and S.A. Nasar, Electrical drives, 2nd ed., CRC, 2005.

[2] Bimal K. Bose, Modern Power Electronics and AC Drives, 4th ed., South Asia: Pearson Prentice-Hall, 2007.

[3] P. Pillay and R. Krishnan, "Modeling of Permanent Magnet Motor Drives", IEEE Trans.Ind. Elect., vol. 35, no. 4, pp. 537-541, November 1988.

[4] R. Krishnan, Electric Motor Drives: Modeling, Analysis, and Control, Prentice-Hall, Upper Saddle River, NJ, 2001.

[5] C. Xia, J. Zhao, Y. Yan and T. Shi, "A novel direct torque control of matrix converter-fed PMSM drives using duty cycle control for torque ripple reduction", IEEE, Trans. Ind. Elect., vol. 61, no. 6, pp. 2700-2713, June, 2014.

[6] M. Preindl and S. Bolognani, "Model predictive direct torque control with finite control set for PMSM drive systems, Part 1: Maximum torque per ampere operation", IEEE Trans. Ind. Informatics, vol. 9**, no: 4**, pp. 1912-1921, November, 2013.

[7] A. Mishra, J. A. Makwana, P. Agarwal, and S.P. Srivastava. "Modeling and implementation of vector control for PM synchronous motor drive", IEEE, Int. Conf., Advances in Engineering, Science and Management (ICAESM)'12, pp. 582- 585, March 2012.

[8] Asri, D. Ishak, S. Iqbal and Moh. Kamarol, "A speed sensorless field oriented control of parallel-connected dual PMSM," IEEE Int. Conf., Control System, Computingand Engineering (ICCSCE)'11, pp. 567-570, November 2011.

[9] A. A. Mahfouz and W. M. Mamdouh, "Intelligent DTC for PMSM drive using ANFIS technique," Int. Journal of Engineering Science and Technology (IJEST), vol. 4, no. 3, pp. 1208-1222, March, 2012.

[10] P. Wood, Theory of Switching Power Converter, New York: Van Nostrand-Reinhold, 1981.

[11] B.-K. Lee and M. Ehsani, "A simplified functional simulation model for three-phase voltage-source inverter using switching function concept", IEEE Trans. Ind. Elect., vol. 48, no: 2, pp. 309-321, April, 2001.

[12] A. Nachiappan, K. Sundararajan and V. Malarselvam, "Current controlled voltage source inverter using hysteresis controller and PI controller," IEEE, Int. Conf., Power, Signals, Controls and Computation (EPSCICON)'12, pp.1-6, January, 2012.

[13] P. H. Zope, P. G. Bhangale, P. Sonare and S. R. Suralkar, "Design and implementation of carrier based sinusoidal PWM inverter," Int. Journal of Advanced Research in Electrical, Electronics and Instrumentation Engineering, vol. 1, no. 4, pp. 230-236, October, 2012.

[14] R. Krishnan, Permanent Magnet Synchronous and Brushless DC Motor Drives, CRC, 2010.

[15] P. Pillay and R. Krishnan, "Modeling, simulation, and analysis of permanent-magnet motor drives, Part I: The permanent-magnet synchronous motor drive", IEEE Trans. Ind. Appl., vol. 25, no. 2, pp. 265-273, March/April 1989.

[16] A. R. Sabitha and S. S. Beevi. "Encoderless vector control of interior PMSM with initial states," Int. Conf. Automation, Computing, Communication, Control and Compressed Sensing, pp. 342-345, March 2013.

[17] E. P.Wiechmann, P. D. Ziogas, and V. R. Stefanovic, "Generalized functional model for three phase PWM inverter/rectifier converters", in Conf. rec. IEEE-IAS Annu. Meeting, pp. 984–993, 1985.

[18] J. Gao and J. Kang, "Modeling and simulation of permanent magnet synchronous motor vector control," Information Technology Journal, vol. 13, no. 3, pp. 578-582, February, 2014.

[19] Y. Yan, J. Zhu, Y. Guo and H. Lu, "Modeling and simulation of direct torque controlled PMSM drive system incorporating structural and saturation saliencies," Ind. Appl. Conf. 41st IAS Annu. Meeting Conf. rec., IEEE, vol. 1, pp. 76-83, October 2006.P. D. Ziogas, E. P.Wiechmann, and V. R. Stefanovic, "A computer-aided analysis and design approach for static voltage source inverter", IEEE Trans. Ind. Appl., vol. IA-21, pp. 1234–1241, September/October, 1985.

[20] M. Rashid, Power Electronics: Circuits, Devices, and Applications, 4th ed., Pearson Education, 2013.

[21] M. Marufuzzaman, M. B. I. Reaz, L. F. Rahman and T. G. Chang, "High-speed current dq PI controller for vector controlled PMSM drive," The Scientific World Journal, pp.1-9, January, 2014.

[22] Peter Vas, Sensorless Vector and Direct Torque Control, Oxford University Press, NY, 1998.

[23] W. R. Liou, H. M. Villaruza, M. L. Yeh and P. Roblin, "A digitally controlled low-EMI SPWM generation method for inverter applications," IEEE, Trans. Ind. Informatics, vol. 10, no. 1, pp. 73-83, February, 2014.

[24] M. Lakka, E. Koutroulis and A. Dollas, "Development of an FPGA-based SPWM generator for high switching frequency DC/AC inverters," IEEE, Trans. Power Elect., vol. 29, no. 1, pp. 356-365, January, 2014.

[25] M. P. Kazmierkowski and L. Malesani, "Current control techniques for three-phase voltage-source PWM converters: a survey," IEEE, Trans. Ind. Elect., vol. 45, no. 5, pp. 691-703, October, 1988.

[26] N. P. Ananthamoorthy and K. Baskaran, "Simulation of PMSM based on current hysteresis PWM and fed PI controller," Int. Conf. Computer Communication and Informatics (ICCCI)'12, pp. 1-5, January 2012.

[27] P. Pillay and R. Krishnan, "Control characteristics and speed controller design for a high performance of permanent magnet synchronous motor drive," IEEE Trans. Power Elect. Vol. 5, no. 2, pp. 151-159, April 1990.

[28] M. A. Khan and M. N. Uddin, "Performance analysis and optimization of digitsl PWM controllers for surface-mounted PMSM drives," IEEE, Industry Applications Society Annual Meeting (IAS)'12, pp.1-8, October, 2012.

APPENDIX

Parameter Values of PMSM used in Simulation

P=6 poles; R_s= 1.4Ω; L_d = 5.6mH; L_q = 9mH; J = 0.006 kgm2; B = 0.01 Nm/rad/s; $\lambda^*_m = \lambda_{af}$ = 0.1546 V/rad/s; ω^*_r = 314.3 rad/s; $T_e^* = T_b$ = 5.5631 N-m; V_{dc}=285 V; Δi=1.2, f_c=20 kHz. These parameters were taken from reference [3].